Journal of Power Sources 268 (2014) 301–314

Contents lists available at ScienceDirect

Journal of Power Sources

journal homepage: www.elsevier.com/locate/jpowsour

Analysis of electric and thermal behaviour of lithium-ion cells in realistic driving cycles

Abbas Tourani [a, *], Peter White [a], Paul Ivey [b]

[a] Faculty of Engineering and Computing, Coventry University, Priory Street, Coventry CV1 5FB, UK
[b] Birmingham City University, City North Campus, Birmingham B42 2SU, UK

HIGHLIGHTS

- A multi-scale thermo electrochemical model for lithium ion cells is developed.
- The test results of lithium-ion cells are presented.
- The operating condition for the best performance of the examined battery cell is identified.
- The results of applying battery cell in a realistic driving cycle is presented.
- A crucial recommendations are suggested for the battery management systems of BEV.

ARTICLE INFO

Article history:
Received 28 February 2014
Received in revised form
1 May 2014
Accepted 3 June 2014
Available online 11 June 2014

Keywords:
Lithium-ion
Driving cycles
Operating temperature
Electric vehicle
Heat generation

ABSTRACT

A substantial part of electric vehicles (EVs) powertrain is the battery cell. The cells are usually connected in series, and failure of a single cell can deactivate an entire module in the battery pack. Hence, understanding the cell behaviour helps to predict and improve the battery performance and leads to design a cost effective thermal management system for the battery pack. A first principle thermo electrochemical model is applied to study the cell behaviour. The model is in good agreement with the experimental results and can predict the heat generation and the temperature distribution across the cell for different operating conditions. The operating temperature effect on the cell performance is studied and the operating temperature for the best performance is verified. In addition, EV cells are examined in a realistic driving cycle from the Artemis class. The study findings lead to the proposal of some crucial recommendation to design cost effective thermal management systems for the battery pack.

1. Introduction

Driving cycles are a standard way to compare the performance of different vehicles. There are two classes of driving cycle, modal cycle such as the new European driving cycle (NEDC) and transient cycle such as the Assessment and Reliability of Transport Emission Models and Inventory systems (Artemis). The NEDC cycle is a compilation of straight acceleration and constant speed periods representing typical driving patterns, and uses to assess the CO_2 and fuel efficiency performance of all passenger vehicles, either internal combustion engines or electric vehicles, in Europe. Whereas transient cycles such as Artemis involve many speed variations, typical of on-road driving conditions and is a statistical representative of real driving cycles.

The study of the driving cycle has applied predominantly at the battery pack level in electric vehicles. Very limited research has looked at the effect of a driving cycle at the cell level. Dubarry et al. built a real life drive cycle and applied a simple empirical battery model [1]. They attempted to provide a coherent approach for a realistic empirical model to simulate battery cell performance, and establish a scheme to better understand and predict battery cell performance. More recently, Klein [2] simplified the first principle models for lithium-ion cells and applied driving cycles to examine the fidelity of the simplified model. However, the thermal issue was not subject of their works. Gerver [3] and co-authors studied large scale batteries (20 × 30 cm size) used under high power conditions, 5 C rate(1 C is a full discharge in 1 h, based upon theoretical capacity, so 5 C is a full discharge in 12 min). They developed a coupled electrochemical battery model with a thermal model to determine temperature distributions throughout the battery. They applied their model to optimise the terminal tab position in the cell

* Corresponding author. Tel.: +44 (0) 247 765 7734.
E-mail address: tourania@coventry.ac.uk (A. Tourani).

http://dx.doi.org/10.1016/j.jpowsour.2014.06.010
0378-7753/

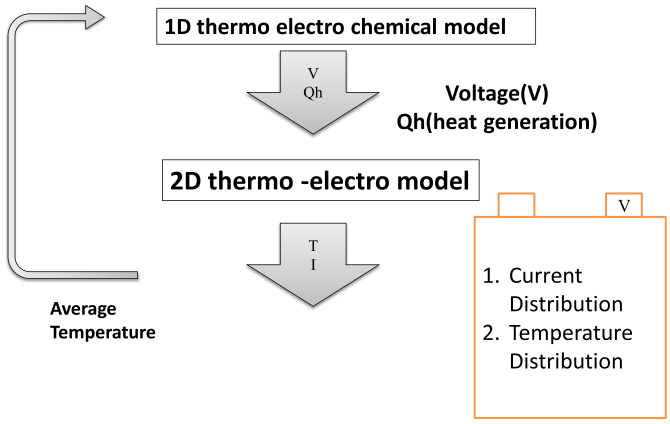

Fig. 1. The model sequence.

and some similar design applications of the cell. However, the model results were compared with the experimental measurements of other researchers [4] and the effect of driving cycles and heat dissipation parameters were not studied. More recently, Xiao [5] and Guo [6] developed dynamic models for a pouch type lithium-ion battery based on electrochemical and thermal principles to analyse performances of a single cell. However, the effect of ambient temperature and driving cycle were not studied in their work. It is concluded that the heat transfer issues of EV battery cells have not been fully incorporated into models so far developed. The heat transfer studies are focused on the battery pack and the issue has not been examined at the fundamental level of EV batteries, the cell.

This paper is a development of a previous paper published by the authors [7] in which the results of study the battery cell behaviour in a typical driving cycle, NEDC were presented. The current paper, by concentrating on the heat transfer study at the cell level, contributes to understanding the cell behaviour under different operating conditions. The authors developed physic based model [8] is applied to verify the operating temperature for the best performance. In addition, the operating temperature effect on the cell performance is studied and the BEV cells are examined in a realistic driving cycle from the Artemis class. The study findings lead to the proposal of some crucial recommendation to design cost effective thermal management systems for the battery pack.

2. The model definition and validation

The model [8], which is applied in this paper, is a physics-based model that consists of two sub-models, the 1D electrochemical sub model, and 2D thermo-electro sub model, which are coupled and solved concurrently. The equations of the model are given in appendix A. The 1D model can predict the heat generation rate (Qh) and voltage (V) of the battery cell through different load cycles. The 2D model of the battery cell accounts for temperature distribution and current distribution across the surface of the battery cell. The battery cell considered is a Lithium Manganese Oxide (LMO) cell of the pouch structure, and the cell is a high capacity cell (20 Ah) dedicated for electric vehicle application.

In terms of the solution sequence, the model input is a load cycle that is representative of the expected drawing down of power/current from the battery cell with time. The 1D electrochemical model for the load cycle, predicts the voltage and state of charge for each components of the cell. The voltage at a point in the 1D model, which corresponds to the tab in the battery cell, and is mapped to the tab position in the 2D model. In addition, the associated total heat generation rate which includes reversible (reaction) and irreversible (Ohmic and overpotential), maps to each computational cells in the 2D model. The 2D model is a thermo-electric model that solves the charge balance (Joule equation) and energy equation concurrently. See Fig. 1. The model results are compared with the experimental results. Fig. 2 shows the model prediction for average temperature of the cell surface and the measurement of average temperature. The differential equation that describes

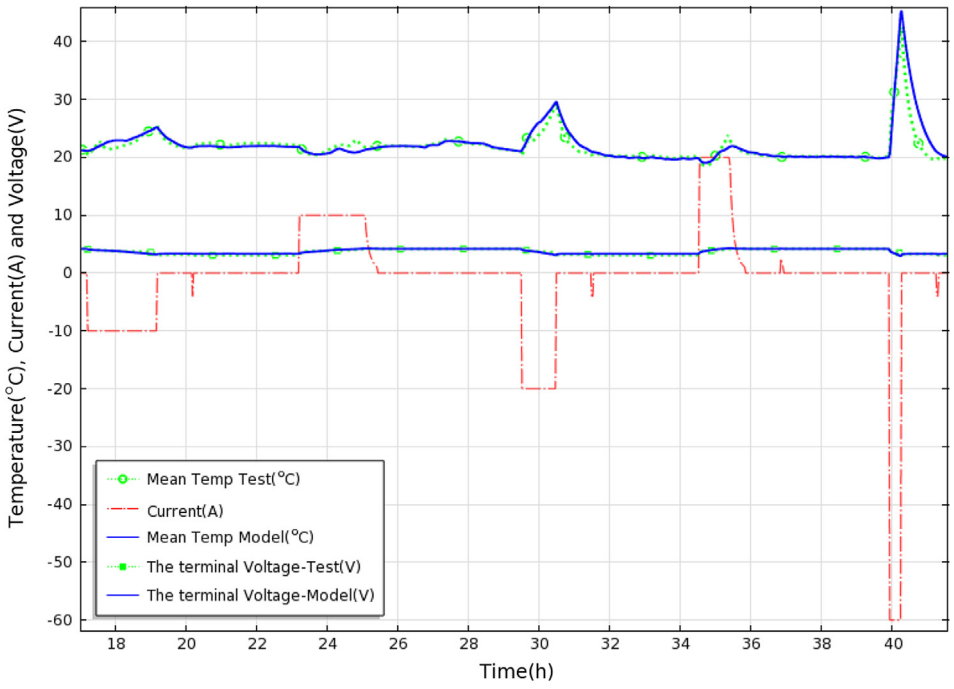

Fig. 2. Comparison between the predicted voltage, temperature of the cell and the test results throughout the load cycle, the nominal capacity of the cell 20 Ah.

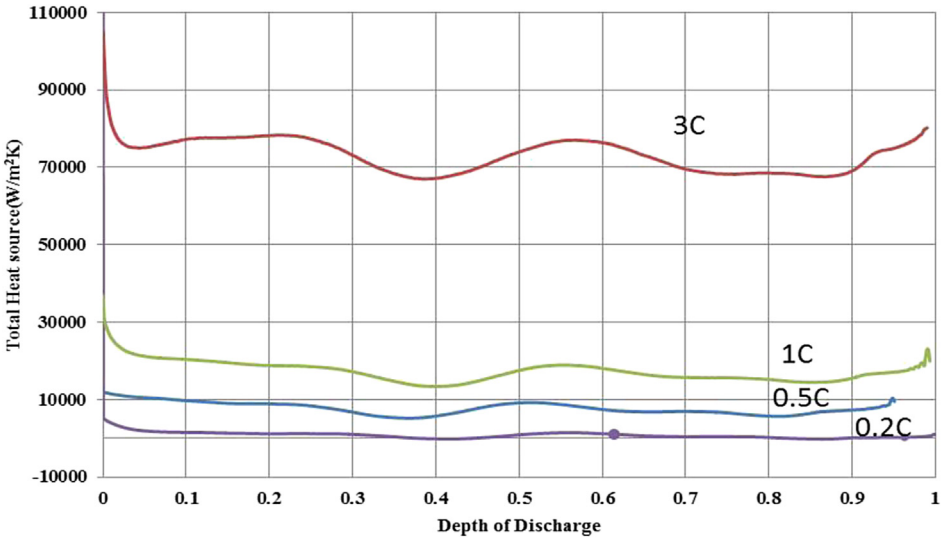

Fig. 3. The total heat sources characteristic obtained by the model at various discharge rates (1C, 20 Ah, the battery cell nominal capacity).

temperature distribution in the battery takes following conservation form

$$\rho c_p \frac{\partial T}{\partial t} = \lambda \nabla^2 T + q_g - q_d \tag{1}$$

q_d is the rate of heat exchanges between the battery cell and surroundings and q_g is the heat source term in the battery cell.

$$q_d = \frac{hA_{cell}}{V_{cell}}(T - T_s) \tag{2}$$

h is the heat transfer coefficient (W m^{-2} K^{-1}),T is the cell temperature and T_s is the surrounding temperature. A_{cell} and V_{cell} are the surface area and volume of the battery cell.

Bernardi [9] governed the complete heat generation term, q_g, and Rao and Newman [10] showed that the heat of mixing in the Bernardi equation is negligible when the open circuit voltage (OCV) of battery does not change rapidly. Therefore, on provision that the reaction distribution is uniform across the porous electrode, and side reactions are negligible, they simplified Bernardi equation [11]. Rao equation has cited frequently in the literature and is applied in the model of this paper. The heat source term (q_g) in the battery cell is defined by Ref. [10]

$$q_g = \sum_j a_{sj} i_{nj}(\varnothing_s - \varnothing_e - U_j) + \sum_j a_{sj} i_{nj} T \frac{\partial U_j}{\partial T} + \sigma^{eff} \nabla\varnothing_s \nabla\varnothing_s + k^{eff} \nabla\varnothing_e \nabla\varnothing_e + k_D^{eff} \nabla \ln c_l \nabla\varnothing_e \tag{3}$$

As stated in Ref. [8], the first term on the right hand side is potential deviation in the control volume from the equilibrium potential (irreversible heat). The second term represents the entropic effects (reversible heat). The third term shows the Ohmic heat in the solid phase and the last two terms represents the Ohmic heats in the solution phase. the thermal conductivity of the battery is anisotropic.

Thermal conductivity in X and Y direction (l_i denotes the thickness of layer i):

$$\lambda = \frac{\sum \lambda_i l_i}{\sum l_i} \tag{4}$$

Thermal conductivity in z direction

$$\lambda_z = \sum \frac{l_i}{\sum \frac{l_i}{\lambda_i}} \tag{5}$$

The heat capacity for the equivalent cell is volume averaged as follows

$$\rho C_p = \sum (\rho C_p)_i l_i \Big/ \sum l_i \tag{6}$$

3. Heat generation in the cell

The model, [8], is applied to verify the heat generation rate at different discharge rates for 0.1 C, 0.3 C, 1 C, and 3 C where C is the nominal capacity of the cell (20 Ah), see Fig. 3. The figure shows the cell operating at high current rate (3 C) results in average heat

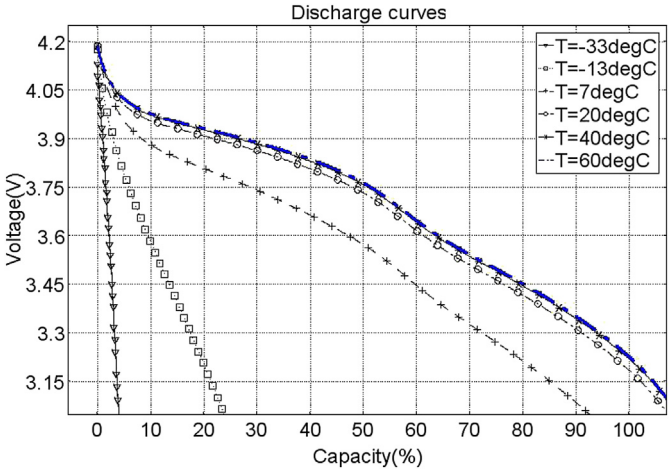

Fig. 4. Voltage curves for the battery cell at 0.3 C discharge rate (6 A) and for different ambient temperatures.

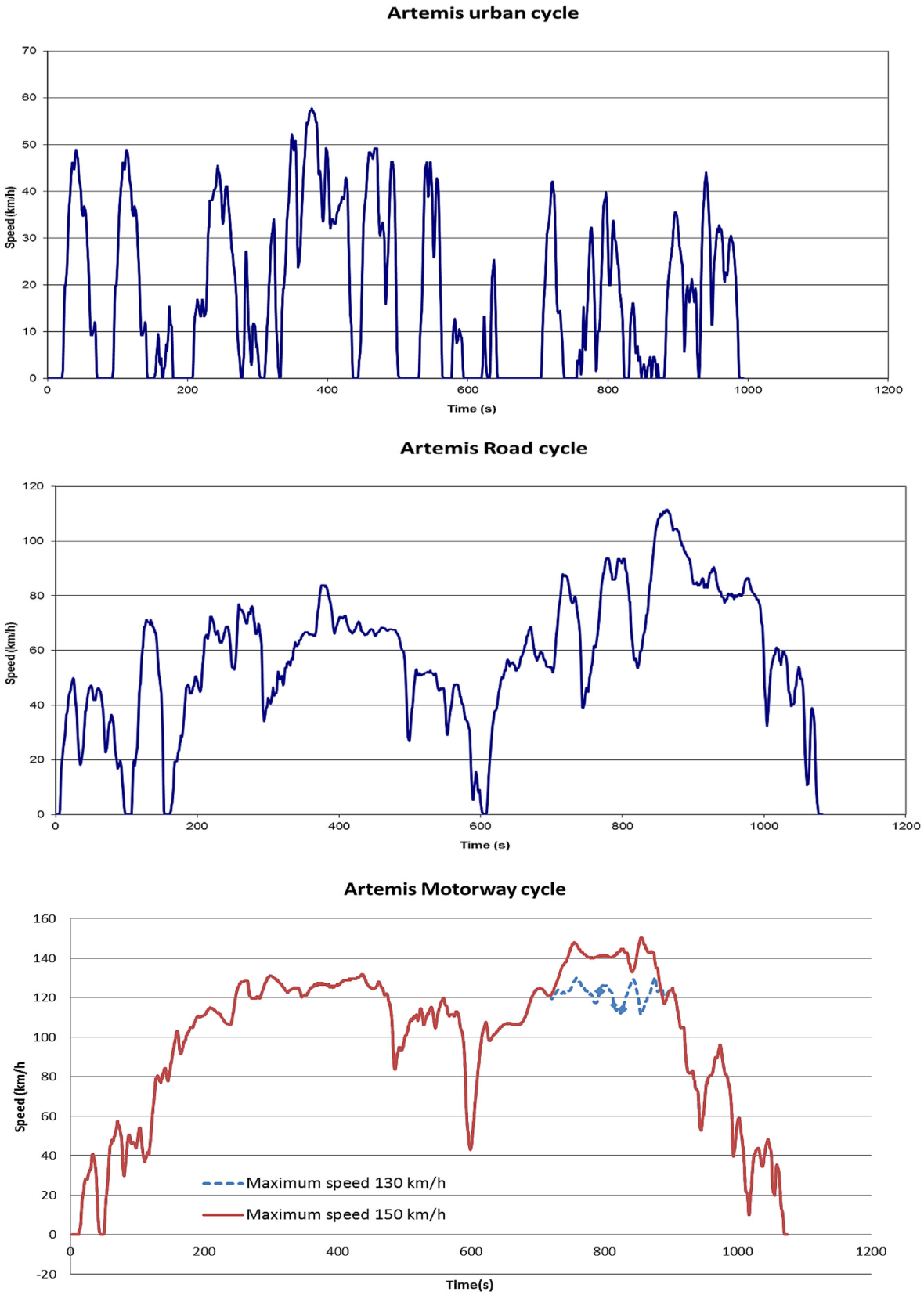

Fig. 5. The Artemis cycles.

Table 1
A typical electric vehicle parameters.

Frontal *l* area of car	2.39	m^2
Percent grade	1	
Vehicle mass	1720	kg
Drivetrain efficiency (inverter to motor)	0.95	
Tyre rolling resistance coefficient	0.015	
Brake and steering resistance	0.003	
Drag coefficient	0.38	
Air density	1.2	kg m^{-3}
Wheel radius	0.3	m
Drag coefficient	0.38	
Air density	1.2	kg m^{-3}
Wheel radius	0.3	m
Battery efficiency (battery to inverter)	0.95	
Gearbox efficiency (motor to wheels)	0.95	
Number of cells	300	
The regenerating coefficient	0.25	
Battery cell capacity	20	Ah
Battery pack energy	25	kWh

generation of 73.2 kW m^{-3} whilst at low current rate (0.2 C) the average heat generation during discharge process is 854 W m^{-3}. One of the key points arising from the results is that the heat source in an EV battery cell is not large enough to satisfy other heating requirement such as cabin heating. However, the heat generation in an EV battery cell application can be managed to maintain the cell at the desired operating temperature in order to improve the performance of the cell. Other source of heating in EVs particularly electrical devices such as an inverter and transistors should also be considered in designing the thermal management system.

4. The operating temperature effect

The lithium-ion cell (LMO) is examined at different operating temperatures. The cell average temperature is considered as a design parameter, which varies from −33 °C to 60 °C. The battery cell performance is expressed by voltage discharge curves when the nominal current (20 A) is drawn from the battery. This cycle is selected as representative of cell performance for different operating temperatures.

As it can be seen in Fig. 4, the operating temperature has significant effect on the voltage–capacity characteristic of the cell. The temperature dependent parameters are valid between −7 °C and 60 °C; however, the model predicts the cell voltage–capacity characteristic at different operating temperature from −33 °C to 60 °C. It is observed that the cell cannot be operated at low temperature as the voltage drops dramatically. For instance, at the operating temperature of −33 °C, the voltage of the battery decreases quickly to the cut off voltage (2.9 V) and only 5% of the capacity of the battery cell can be drawn down. The main reason for performance dropping is the reduced rate of the chemical reaction associated with the mass transfers.

At high temperature, faster chemical reactions occur and the cell delivers constant voltage throughout the discharge cycle. As Fig. 4 shows, increasing the operating temperature from 20 °C to 60 °C did not have a significant effect on the voltage–capacity characteristic. In addition, the high operating temperatures cause thermal stress within the cell [12]. Therefore, an upper operating temperature limit for the cell should be considered. In order to optimise the performance, and according to the results of the operating temperature effect study, the cell requires a working temperature range of 20 ± 5 °C and the cell should not encounter high temperature differences.

5. Drive cycle study

The fuel consumption and pollutants emissions of conventional internal combustion cars are assessed using standard modal driving cycles such as the new European driving cycle (NEDC). The results of studying the cell in NEDC cycle was presented in the previous paper published by the authors [7]. Car manufacturers use realistic driving cycle such as Artemis cycle to better understanding real driving conditions and evaluate real performances of their vehicles. The Artemis cycle consists of 3 different configurations, plus an additional variant. These are the urban cycle, the road cycle, the motorway 130 km h^{-1} and the motorway 150 km h^{-1}, see Fig. 5.

The model is applied to investigate the battery cell behaviour associates with realistic driving cycles. Typical electric vehicle parameters are considered to determine the power required from battery cell. The effects of three configurations of Artemis cycles are studied separately and a combined motorway and urban cycle is also studied, and further the effect of ambient temperature and heat transfer coefficient are discussed.

Based on the basic formulae for the physics of motion and for the typical battery electric vehicle parameters, Table 1, the power required from the battery cell associated with the Artemis cycle load is calculated. The detail of the calculation is described in Appendix B.

The power required from the battery cell, voltage and mean temperature for an hour journey on the Artemis urban cycle and half an hour journey on the Artemis road cycle are shown in Figs. 6 and 7. The average temperature and voltage of the battery cell are obtained at different ambient temperatures with the range from −10 °C to 35 °C.

A typical electric vehicle is considered to apply 25% of deceleration power to charge the battery, [13] and the results show that the battery cell is not fully discharged either at the end of an hour urban Artemis or half an hour Artemis road journey. This finding can contribute in estimating BEV mileage and demonstrates the effectiveness of BEV application for commuting trips. Since a report from "Element Energy" [14] identifies commuting as accounting for 25% of total annual car miles, and around two thirds of commuting trips are less than ten miles long. This means that the battery cell and consequently the battery electric vehicle can achieve the majority of commuting trips without being fully discharged. In addition, electric vehicles can apply ultra-capacitors [15] or range extender technologies to increase the power capability or extend the range.

The results of Figs. 6 and 7 show that the cell temperature is dominated by the ambient temperature in both urban and road cycles. The cell temperature at the end of the journey reaches the ambient temperature whether the ambient temperature is less or more than the initial temperature of the cell, 20 °C. This is assuming a heat transfer coefficient of $h = 6$ W m^{-2} K^{-1} for edges and large surfaces of the cell. This heat transfer coefficient can be obtained from the different methods of heat transfer, convection, conduction and radiation. This finding can lead to verify the objective of the thermal management; as it would be concentrating on insulating the cell from adverse ambient temperature.

The cell behaviour is also studied for a half an hour journey on the motorway Artemis cycle; Fig. 8. The results are in agreement with the results of using the battery cell in urban and road Artemis cycles as the cell is not fully discharged at the end of journey and the cell temperature is again dominated by ambient temperatures. However since the voltage decreases to the cut off voltage, the cell could not manage to last longer than half an hour journey with Artemis motorway cycle. In addition, the cell temperature rises above the ambient temperature and the configured thermal mass

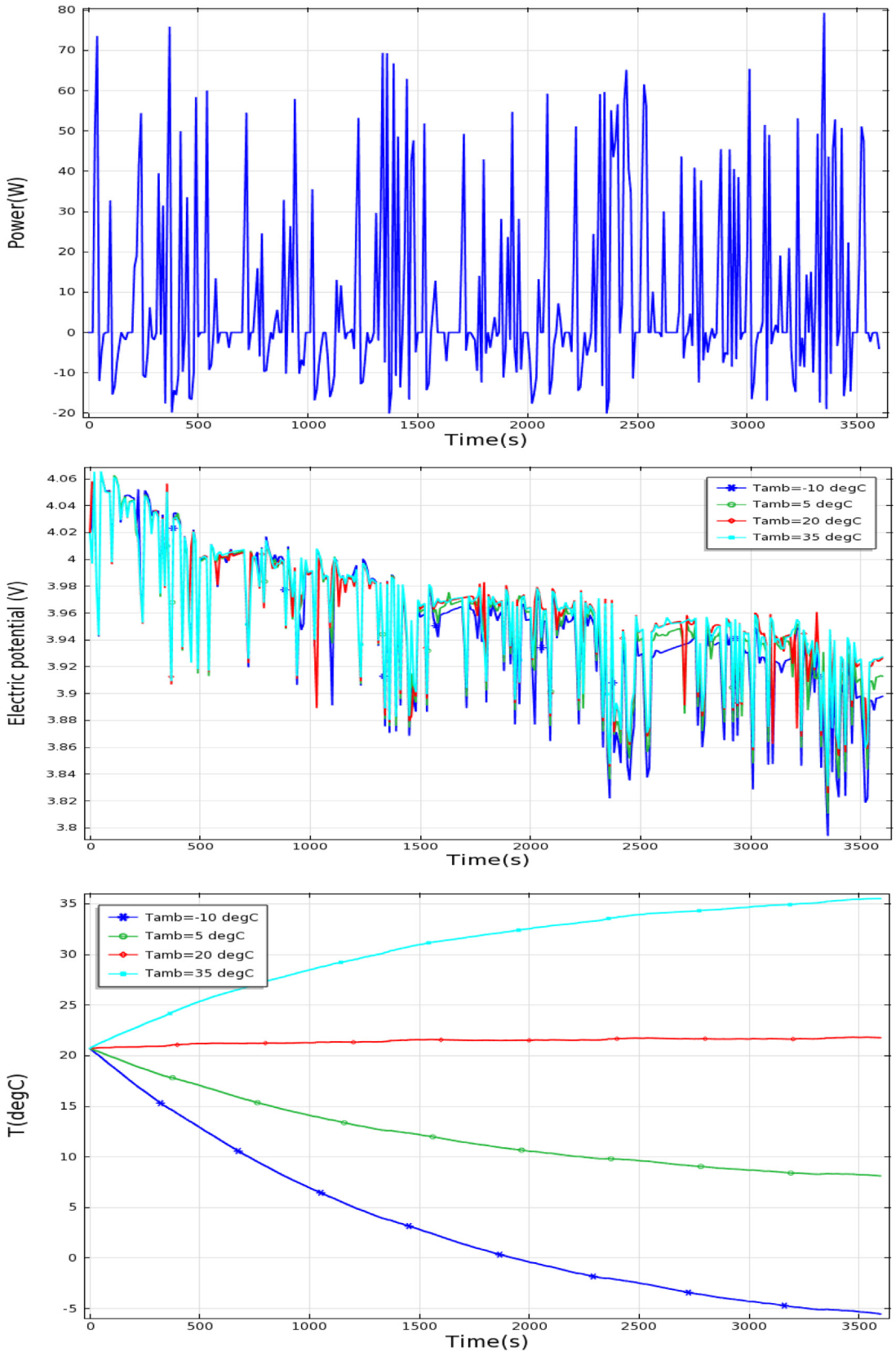

Fig. 6. The battery cell required power, voltage and mean temperature in an hour journey with Artemis urban cycle for different ambient temperatures.

and heat dissipation rates could not balance with the heat generation rates.

In order to investigate the battery cell behaviour in a realistic journey between two cities, a typical combined journey within Artemis motorway and urban cycles is considered. It is assumed that the journey is combination of 6 min urban driving, maximum speed 50 km h^{-1}, followed by 18 min motorway driving, maximum speed 120 km h^{-1}, and 6 min urban driving. The power required, voltage and average temperature of the battery cell are shown in Fig. 9.

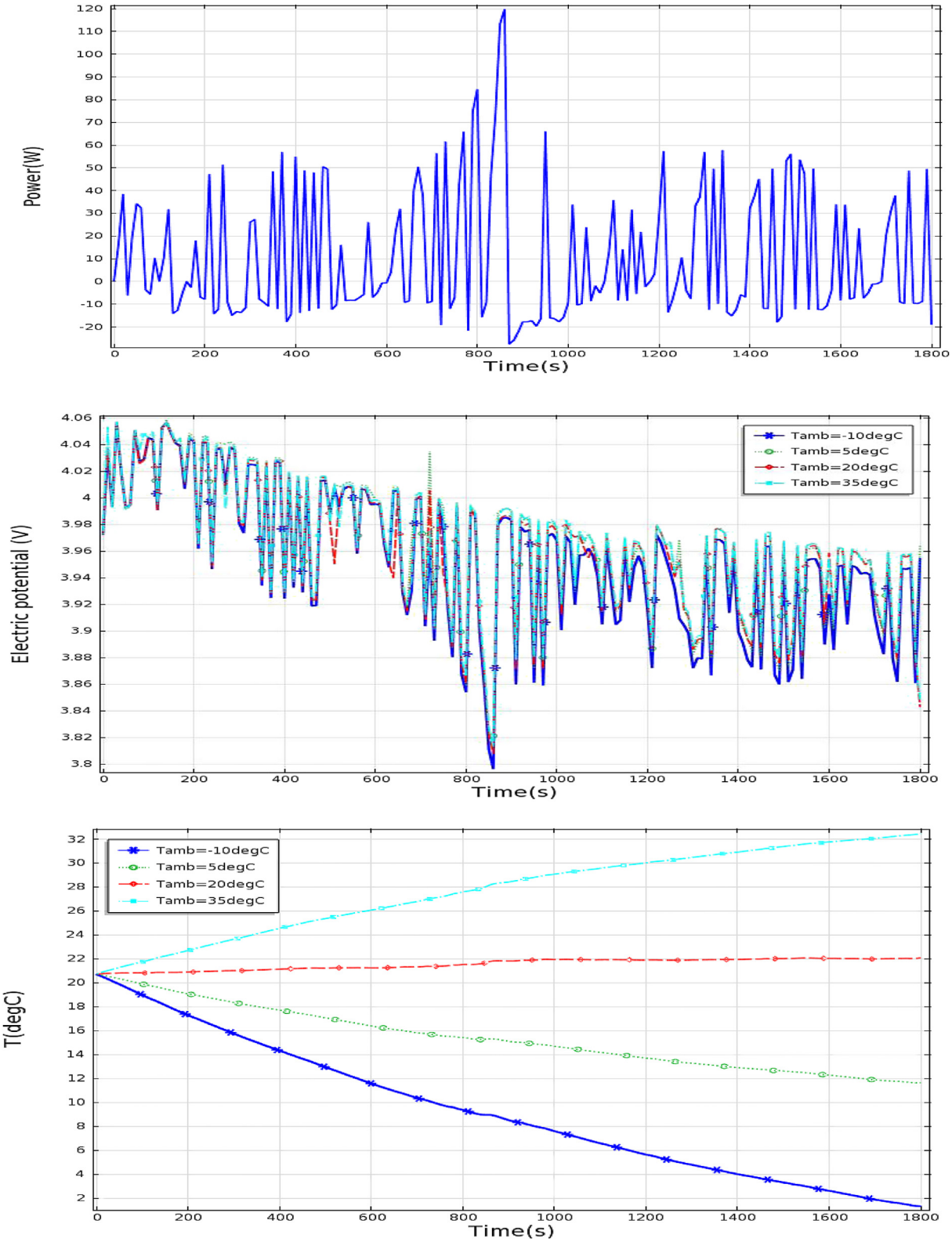

Fig. 7. The battery cell required power, voltage and mean temperature for a half an hour journey with Artemis road cycle for different ambient temperatures.

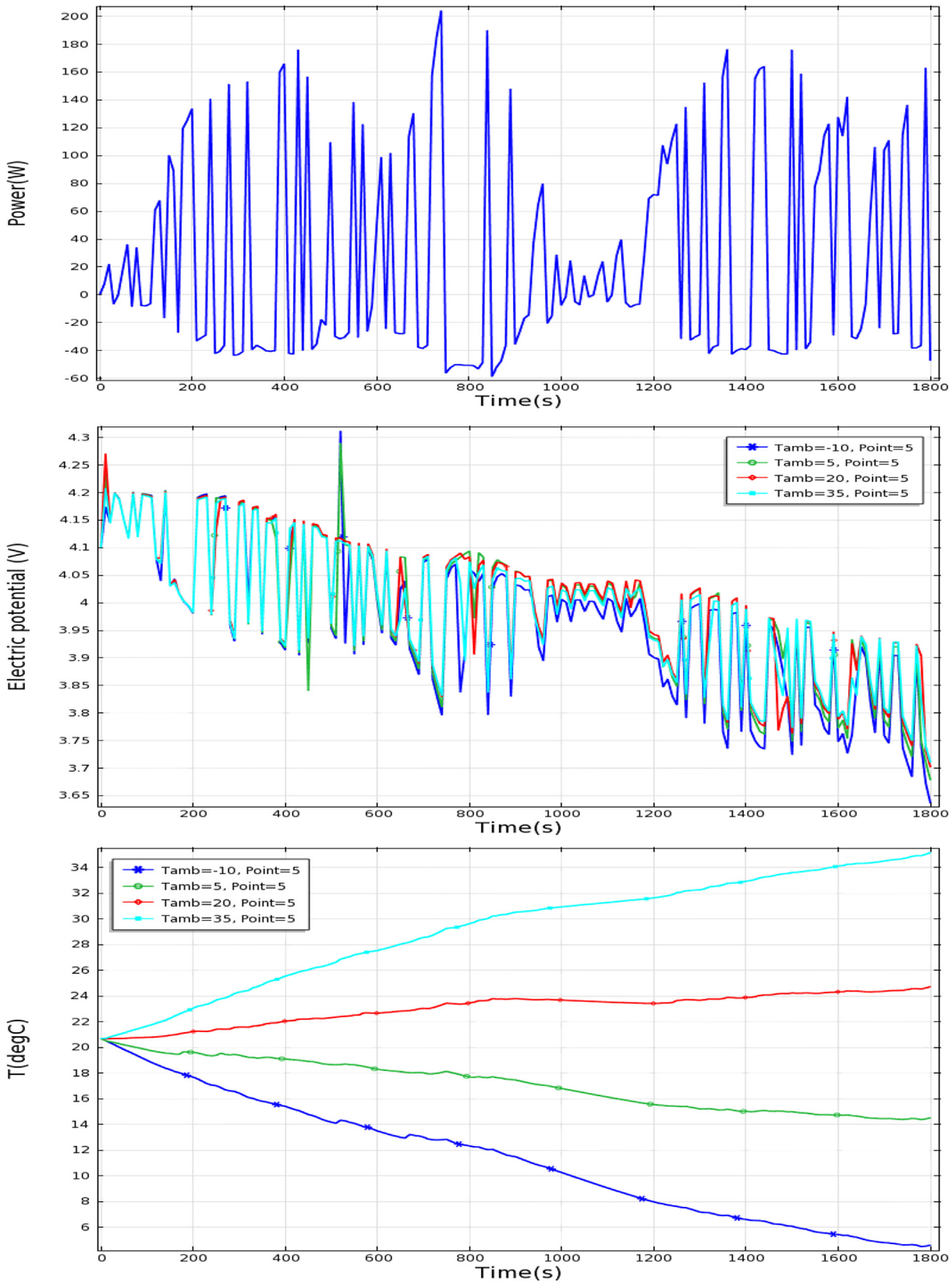

Fig. 8. The battery cell required power, voltage and mean temperature in half an hour journey with Artemis Motorway cycle for different ambient temperatures.

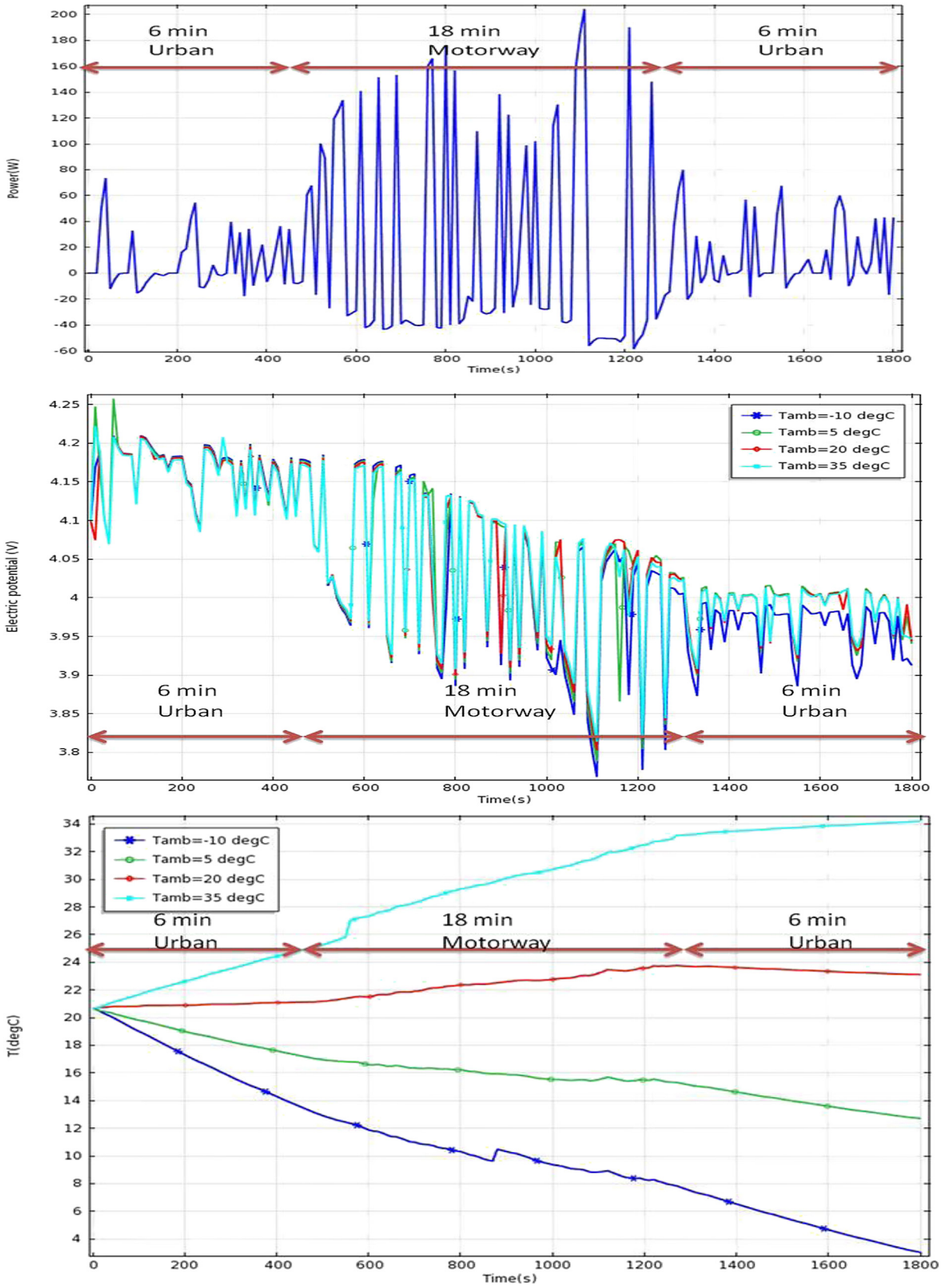

Fig. 9. The battery cell required power, voltage and mean temperature in half an hour combined cycle (Artemis Motorway and Urban cycles) for different ambient temperatures.

The results show the voltage and average temperature of the cell change in a way to reach the ambient temperatures for the first 6 min of the urban cycle, then the voltage drops and temperature rises up gradually through the motorway cycle. The journey ends up with 6 min urban cycle during which the cell temperature falls down to the ambient temperature.

The study again shows the effect of the ambient temperature and highlights that the heat dissipation rate should be increased in

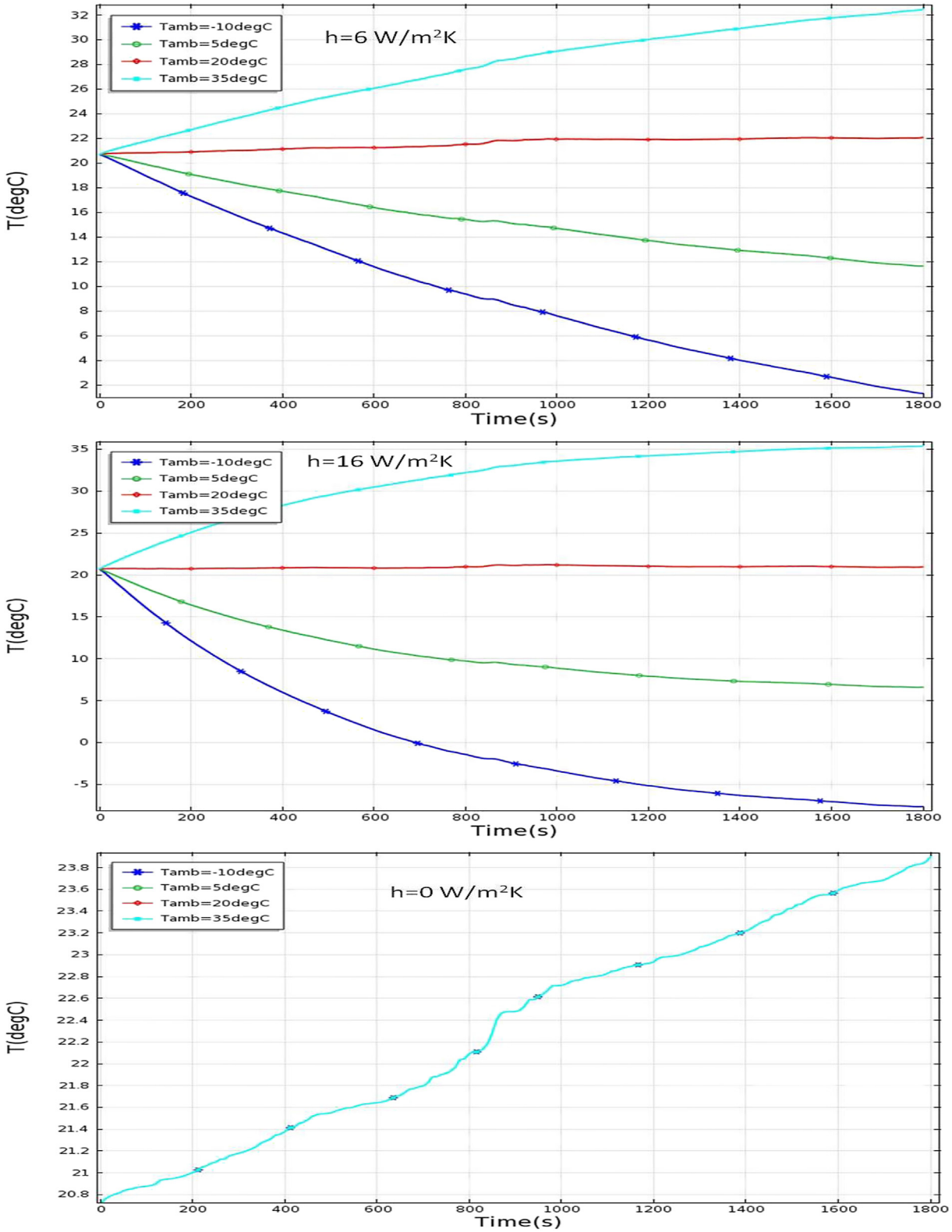

Fig. 10. The battery cell mean temperature in half an hour Artemis Road cycle with constant heat transfer coefficients and different ambient temperature.

motorway segment of the cycle. This finding leads to designing the thermal management of BEV cells in a way to provide variable heat dissipation rates depending on the heat generating rates and the ambient temperatures.

6. The heat transfer study

Battery cells depending on their position in the battery pack might have different heat transfer coefficients, and surrounding conditions. In this study, different possible heat dissipation conditions are considered for a particular battery cell, which in comparison with thermal studies of a battery pack are less complex, and lead to lower solution times and cost. Instead, the multi physics based model for different load conditions predicts the heat generation term. The heat transfer coefficient is considered as a design parameter with the range 0, 6, 16 W m^{-2} K^{-1}, and the cell behaviour at different ambient temperature and heat transfer coefficients is studied. The heat transfer coefficient of zero corresponds to an adiabatic condition in which the battery cell is assumed to be insulated from the surrounding. The heat transfer coefficient of 6 W m^{-2} K^{-1} corresponds for a passive cooling with a buoyancy flow around the battery cell, and the highest heat transfer coefficient represents active cooling with a forced flow around the battery cell. The Artemis road cycle with the average speed of 57 km h^{-1} is considered as the load cycle and the results are shown in Figs. 10 and 11. The temperature of surroundings or equally a coolant temperature can represent the cell ambient temperature, if active cooling is applied.

Fig. 10 shows the results of using different heat transfer coefficients within the constant ambient temperatures. It is observed when the cell is in the adiabatic condition, $h = 0$ W m^{-2} K^{-1}, the cell temperature eventually increases by 3 °C in 30 min regardless the variation of the ambient temperature. The cell in the adiabatic condition with the considered thermal inertia would cope with the amount of heat generated throughout the cell.

As the cell begins to transfer heat with the surrounding, $h = 6$, 16 W m^{-2} K^{-1} in Fig. 10, the cell experiences higher temperature

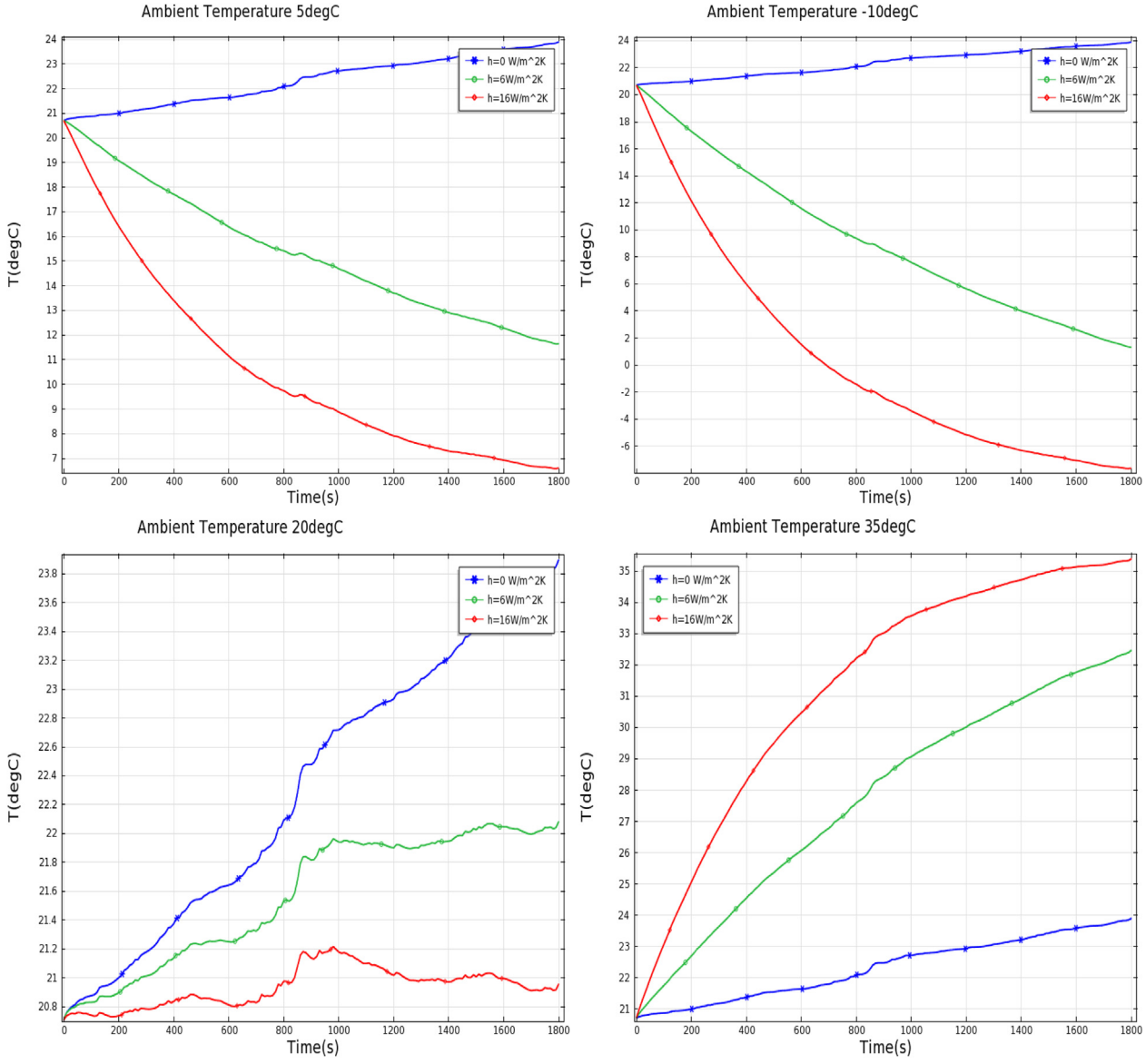

Fig. 11. The battery cell mean temperature in 30 min Artemis Road cycle with different heat transfer coefficients and constant ambient temperature.

gradient than the adiabatic conditions and this gradient depends on the ambient temperature. For example, the cell with the highest heat transfer coefficient, 16 W m^{-2} K^{-1}, and the lowest ambient temperature,−10 °C, has the temperature difference of 30 °C throughout the half an hour journey with Artemis road cycle.

The results for the upper limit of the heat transfer coefficient, 16 W m^{-2} K^{-1} in Fig. 10, shows that with this heat transfer coefficient, and the assumed thermal mass of the cell, the cell temperature is dominated by the ambient temperatures. On the other hand, the thermal inertia of the cell is considered as a constant parameter that can be a function of temperature or state of charge. Although this assumption is a well-accepted for researches on the cell level [16], this is should be verified experimentally.

The studies of using different ambient or coolant temperatures are shown in Fig. 11. The ambient temperature varies from −10, 5, 20, 35 °C. For the ambient temperature of 20 °C, using the high heat transfer coefficient helps to reduce the temperature difference throughout the cycle and it appears the difference drops from 3 °C in adiabatic condition to 1 °C when the heat transfer coefficient is 16 W m^{-2} K^{-1}. However, it would not be a cost effective approach to apply high heat transfer coefficient at this ambient temperature. Conversely results have been shown when the ambient temperatures are −10, 5, 35 °C using the high heat transfer coefficient of 16 W m^{-2} K^{-1} increases the cell temperature difference from 4 °C in the adiabatic condition to 15 °C when the ambient temperature is 35 °C. This finding shows that the optimum coolant temperature can be 20 °C when the ambient temperature is not equal to this temperature.

7. Conclusion

A first principle model is applied to study the lithium-ion (LMO) cell behaviour at different operating conditions. The results show that below an operating temperature of 7 °C, a common ambient temperature in a Northern European winter, the cell performance falls off dramatically, whereas there is little or no gain in the performance above 27 °C. Further, the lithium-ion cell (LMO) is examined in Artemis realistic driving cycles, and the effect of ambient temperature on the cell behaviour during the driving cycles is studied. The results show the BEV cell temperature in the urban cycle is a function of ambient temperature, and the main thermal concern in the urban driving cycle is to maintain the cells in an optimum working temperature envelope (20 ± 5 °C).

As the BEV cell needs to draw less than a 1 C discharge rate in urban cycles, the cell can dissipate the heat through natural convection. However, the cell experiences a rising temperature when drawing more than 3 C discharge during high speed driving or acceleration. An active cooling system will be needed in this case to reduce the temperature. In addition, the results highlight the role of a maximum power limit on the cell temperature, which can be minimised to reduce the need for thermal management. Further analysis is needed to determine the optimum number of cells to reduce the power limit, minimise the cost, weight, size, and thermal management cost of the battery pack.

The results of studying the effect of heat transfer coefficients show that when the cell is in an adiabatic condition, the cell temperature eventually rises 3 °C regardless of the variation in the ambient temperature. The cell temperature at the end of the journeys approaches the ambient temperature whether the ambient temperature is less or more than the initial temperature of the cell, 20 °C. These findings show the main thermal issue of an urban BEV cell is insulating the cell from adverse ambient temperature. In addition, high heat transfer coefficients particularly in a low temperature surrounding would result in cooling of the cell.

In summary, this paper presents thermal behaviour study of a battery cell, which is the preliminary and essential study to design a thermal management system for a battery pack, and helps to understand the scope of the thermal problem within the battery cell. The knowledge could apply to configure the battery module and pack in a way to reduce the cost and weight of thermal management systems of BEVs. The cell model is planned to contribute in a BEV thermal management systems model as proposed by Ref. [17] in a way that the cell level model will be developed by an assembly of ten cells with integration of cooling system.

The findings of the project give a methodology for determining the heat generation and temperature distribution within lithium-ion cells in a BEV, and introduce a new hypothesis to design a thermal management system for BEV batteries. The thermal management system should be designed in a way to maintain, for the cell under consideration, a varying temperature of 20 ± 5 °C whatever the ambient conditions.

It is recommended that the study of heat generation and dissipation in EV cells in battery packs is continued and the performance of thermal management techniques to maintain the cell in the required operating range are compared. For example, phase change materials [18] and heat pipes [19] have been introduced recently to the thermal management of BEVs, and the model can be modified to include these passive cooling methods. In addition, the ways to provide a coolant in an active thermal managements system with low temperature variation should be studied.

Appendix A. The model electrochemical equations

List of symbols

c_1	Concentration of the electrolyte (mol m^{-3})	T	Temperature (K)
c_s	Surface concentration in spherical particle (mol m^{-3})	F	Faraday's constant (C mol^{-1})
C_p	Specific heat (J kg^{-1} K^{-1})	f	Ionic activity coefficient
j_{loc}	Transfer current density (A m^{-2})	t_+	Transport number
q	Volumetric heat generation rate (J m^{-3} s^{-1})	ε	Porosity (volume fraction of electrolyte)
U_j	Equilibrium potential (V)	D_l^{eff}	Effective diffusivity in the electrolyte (m^2 s^{-1})
k^{eff}	Effective solution conductivity (Ω^{-1} m^{-1})	i_0	Exchange current density (A m^{-2})
λ	Thermal conductivity (W m^{-1} K^{-1})	E_{ref}	Electrode particle's equilibrium potential (V)
ρ	Density (kg m^{-3})	$c_{1,\,surf}$	Particle surface concentration (mol m^{-3})
σ_{eff}	Effective matrix conductivity (Ω^{-1} m^{-1})	k_0	reaction rate constant
Φ_1	Potential in the matrix phase (V)	$c_{1,\,max}$	Maximum surface concentration (mol m^{-3})
Φ_2	Potential in the solution phase (V)	η	Activation overpotential (V)
k	Electronic conductivity (S m−1)	D_1	Electrolyte salt diffusivity (m^2 s^{-1})
S_a	Specific surface area (m^2 m^{-3})	$\partial \ln f / \partial \ln c_1$	Activity dependence
R	Gas constant J/(mol K)	D_{sn}	Negative electrode intercalation diffusivity (m^2 s^{-1})
y	Fraction of lithium in the positive electrode	$U_{ref,}$	Open potential of the electrode (V)
γ	Bruggeman coefficient	x	Fraction of lithium in the negative electrode

$$\nabla(-k_l \nabla\phi_l) = -S_a j_{loc} \tag{A-1}$$

$$\nabla\left\{ -k_2^{eff}\nabla\phi_2 + \frac{2RTk_2^{eff}}{F}\left[1+\frac{\partial \ln f}{\partial \ln c_l}\right][1-t_+]\nabla(\ln c_l)\right\} = S_a j_{loc} \tag{A-2}$$

$$y^2 r_p \frac{dc_l}{dt} + \partial\left(-y^2 \frac{D_1}{r_p}\frac{\partial c_s}{\partial y}\right) = 0 \tag{A-3}$$

$$\varepsilon\frac{dc_l}{dt} + \nabla\left\{ -D_l^{eff}\nabla c_l - \frac{i_2}{F}(1-t_+)\right\} = 0 \tag{A-4}$$

$$j_{loc} = i_0\left\{\exp\left(\frac{\eta F}{RT}\right) - \exp\left(-\frac{\eta F}{RT}\right)\right\} \tag{A-5}$$

where

$$\eta = \phi_1 - \phi_2 - E_{ref}(c_l, surf) \tag{A-6}$$

$$i_0 = k_0\sqrt{c_l\left(c_{s,max} - c_{s,surf}\right)c_{s,surf}} \tag{A-7}$$

$$k_i^{eff} = k_i\varepsilon^{\gamma}, \quad i = 1,2 \tag{A-8}$$

$$D_i^{eff} = D_i\varepsilon^{\gamma}, \quad i = 1,2 \tag{A-9}$$

$$U_{ref,n}[20] = -0.16 + 1.32\exp(-3x) + 10\exp(-2000x) \tag{A-10}$$

$$U_{ref,p}[21] = -23.53y^5 + 52.43y^4 - 44.86y^3 + 18.4y^2 - 3.35y + 3.16 \tag{A-11}$$

From Ref. [22]

$$k_l = 0.0001c_l\left(-10.5 + 0.668\times10^{-3}c_l + 0.494{*}10^{-6}c_l^2 + 0.074T - 1.78\times10^{-5}c_l\times T - 8.86\times10^{-10}c_l^2 \times T - 6.96\times10^{-5}T^2 + 2.8\times10^{-8}c_l\times T^2\right)^2 \tag{A-14}$$

$$D_l = 10^{-4}\times10^{-4.43-\left(\frac{54}{T-229-5\times10^{-3}c_l}\right)-0.22\times10^{-3}c_l} \tag{A-15}$$

$$D_{sn} = 1.4523\times10^{-13}\exp\left(\frac{68025.7}{8.314472}\left(\frac{1}{318}-\frac{1}{T}\right)\right) \tag{A-16}$$

Appendix B. Calculating the power required from a battery cell

Three major forces which resist a vehicle from moving are: rolling resistance, aerodynamic drag and the force of gravity as a vehicle moves up a hill. These forces are calculated and the battery cell required power from the cell is estimated for a typical electric vehicle, Table 1. In addition, 25% of the total required power is considered to recharge the battery during deceleration [13]

$$F_{roll} = \mu_{roll} Mg \tag{B-1}$$

F_{roll}: the rolling force
μ_{roll}: the rolling resistance coefficient
M: the mass of the vehicle (kg)
g: the force of gravity (9.8 m s^{-2})

$$D = 1/2\, C_d\, A\, \rho\, V^2 \tag{B-2}$$

D: the drag force
C_d: the Drag coefficient
A: the frontal area of the car (m^2)
ρ: the density of the air (kg m^{-3})
V: the speed of the vehicle (m s^{-1})
The force required to move uphill is a function of the hill angle

$$F_{hill} = (\%\ \text{grade of hill})Mg \tag{B-3}$$

$$\left(\frac{dU}{dT}\right)_n = 344.1347148\exp(-32.9633287x + 8.316711484)/(1 + 749.0756003\exp(-34.7909964x + 8.887143624)) - 0.8520278805x + 0.36229929x^2 + 0.2698001697 \tag{A-12}$$

$$\left(\frac{dU}{dT}\right)_p = \left(4.131274309\exp(0.571536523y) + 1.281681122\sin(-4.9916739y) - 0.090453431\sin(-20.9669665y + 12.5788250) - .0313472974\sin(31.7663338y - 22.4295664) - 4.14532933 + 8.147113434y - 26.064581y^2 + 12.7660158y^3 - 0.184274863\exp(-(y - 0.5169435168)/0.04628266783)^2\right) \tag{A-13}$$

The power required to move a vehicle, P_m, at a certain speed is calculates by

$$P_m = (F_{roll} + D + F\_hill)V \quad \text{(B-4)}$$

The power required to accelerate, P_a, from the speed of V_1 to V_2 in the time interval, t, is calculated by the kinetic energy equation.

$$P_a = \frac{M\left(V_2^2 - V_1^2\right)}{2t} \quad \text{(B-5)}$$

The total power is the summation of the acceleration and movement powers.

References

[1] M. Dubarry, V. Svoboda, R. Hwu, B.Y. Liaw, J. Power Sources 174 (2007) 366–372.
[2] R. Klein, N.A. Chaturvedi, J. Christensen, J. Ahmed, R. Findeisen, A. Kojic, IEEE Trans. Control Syst. Technol. 21 (2013) 289–301.
[3] R.E. Gerver, J.P. Meyers, J. Electrochem. Soc. 158 (2011) A835–A843.
[4] J. Shim, K.A. Striebel, J. Power Sources 119–121 (2003) 955–958.
[5] M. Xiao, S. Choe, J. Power Sources 218 (2012) 357–367.
[6] M. Guo, R.E. White, J. Power Sources 221 (2013) 334–344.
[7] A. Tourani, P. White, P. Ivey, in: Institution of Mechanical Engineers – VTMS 2011, Vehicle Thermal Management Systems Conference Proceedings, 2013, pp. 279–292.
[8] A. Tourani, P. White, P. Ivey, J. Power Sources 255 (2014) 360–367.
[9] D. Bernardi, E. Pawlikowski, J. Newman, J. Electrochem. Soc. 132 (1985) 5.
[10] L. Rao, J. Newman, J. Electrochem. Soc. 144 (1997) 2697–2704.
[11] W.B. Gu, C.Y. Wang, J. Electrochem. Soc. 147 (2000) 2910–2922.
[12] K.E.T. John Newman, Electrochemical Systems, third ed., 2004.
[13] M. Åhman, Energy 26 (2001) 973–989.
[14] C. Cluzel, C. Douglas, Final Report for the Committee on Climate Change, Element Energy Limited, UK, 2012, pp. 1–100.
[15] A. Burke, M. Miller, E. Van Gelder, in: 23rd Int. Electric Vehicle Symposium and Exposition, EVS 2007 ,Conf. Proc. – Sustainability: the Future of Transportation, vol. 4, 2007, pp. 2171–2184.
[16] T.M. Bandhauer, S. Garimella, T.F. Fuller, J. Electrochem. Soc. 158 (2011) R1–R25.
[17] S. Jagsch, C. Kussmann, Thermal System Efficiencies Summit, SAE-2009-01-3078, 2009.
[18] R. Sabbah, R. Kizilel, J.R. Selman, S. Al-Hallaj, J. Power Sources 182 (2008) 630–638.
[19] Z. Rao, S. Wang, M. Wu, Z. Lin, F. Li, Energy Convers. Manag. 65 (2013) 92–97.
[20] L. Cai, Y. Dai, M. Nicholson, R.E. White, K. Jagannathan, G. Bhatia, J. Power Sources 221 (2013) 191–200.
[21] C. Wang, A.M. Sastry, J. Electrochem. Soc. 154 (2007) A1035–A1047.
[22] V. Srinivasan, C.Y. Wang, J. Electrochem. Soc. 150 (2003) A98–A106.